Unsteady flow around a NACA0021 airfoil beyond stall at 60° angle of attack

R. ELAKOURY[1], M. BRAZA[1], Y. HOARAU[2], J. VOS [3], G. HARRAN[1], A. SEVRAIN[1]

[1] *Institut de Mécanique des Fluides de Toulouse, CNRS/INPT UMR N° 5502*
Av. du Prof. Camille Soula, 31400 Toulouse, France

[2] *Institut de Mécanique des Fluides et des Solides de Strasbourg,CNRS/ULP UMR N° 7507*
2 rue Boussingault, 67000 Strasbourg, France

[3] *Computational Fluids and Structures Engineering, Lausanne, Switzerland*

Abstract. The flow around thick and symmetric NACA0021 airfoil at angle of attack 60°, is studied at the Reynolds number based on the chord length $Re = \frac{U_\infty C}{\nu} = 2.7 \times 10^5$. Hybrid Detached Eddy Simulation (DES) approaches are used, with improvement by means of Organised Eddy Simulation (OES) in the context of the URANS part.

Key words: DES, OES, NACA0021 at 60°

1. Introduction

There is a great deal of studies devoted to the prediction of massively unsteady flows around bodies by using URANS or hybrid turbulence approaches. It is well known that the standard URANS approaches are not sufficient to capture correctly the flow unsteadiness. In fact, the strongly detached flow regions and the near-wake coherent structure formation drastically modify the inertial range energy spectrum, comparing to the equilibrium turbulence. These facts have been quantified by means of time-resolved PIV studies carried out in our research group (Braza et al. [3]) that allowed reconsideration of the turbulence scales due to the interaction among the coherent motion and the random turbulence in the context of the OES (Organised Eddy Simulation) approach. A reduction of the turbulence length scale is achieved by the IMFT works in the spectral interaction region that yields a reconsideration of the eddy-diffusion coefficient in the inertial range concerning two-equation modelling, as well as the turbulence damping function. This yields an improved behaviour of two-equation modelling, as discussed in the present paper. The reduction of the turbulence length scale in wall flows with coherent structures and the consequent diminishing of the eddy-diffusion coefficient C_μ in two-equation modelling have been also obtained by means of the second-order closures in URANS (Bouhadji et al [2]). In the present study, the length scale modification has been used furthermore to improve the URANS part of the DES approach. The results are discussed comparing with the standard URANS approach.

2. Turbulence modelling

Turbulence motion in unsteady flows involves organised modes (coherent motion) interacting non-linearly with the fine scale turbulence. This interaction can be studied by means of the turbulence energy spectrum in the inertial range. Indeed, the organised structures display well distinct frequency peaks in the low and the moderate frequency range. The turbulence spectrum undergoes a shape and slope modification from the equilibrium value ($-5/3$) in the vicinity of the organised motion peaks. This has been quantified either by means of the LDV data Djeridi et al., [5], or by time-dependent PIV data, Braza et al. [3], figure 1.

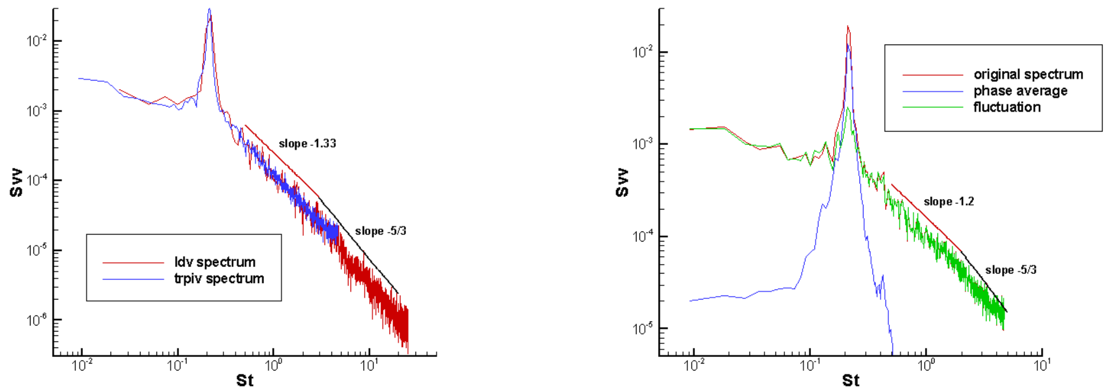

a) b)

Figure 1. Turbulence spectra in the detached flow past a cylinder at $Re = 140000$, ($x/D = 1$, $y/D = 0.375$), showing the slope modification in the inertial range due to interaction between the coherent structures and random turbulence; a) LDV (Djeridi et al., [5]) and PIV turbulence spectra; b) Time-resolved PIV spectrum (Braza et al. [3])

By using a two-component spectral splitting, it can be derived that the turbulence length scale undergoes a significant reduction in the non-equilibrium regions characterised by this slope modification, (Hoarau et al. [7]). An analysis of the scales in the spectral domain yields the same order of magnitude for the eddy-diffusion coefficient. Taking into account these modifications, the nonlinear transfer of energy has been quantified in an analogous way as adopted from the Kovasznay hypothesis (Hinze [6]). The turbulence kinetic energy spectrum, in case of equilibrium takes the form:

$$E\left(\kappa(n)\right) = \left(\gamma_\kappa \alpha_n\right)^{-(2/5).(5/3)} \left[1 - \kappa(n-1)/\kappa(n)\right] (-5/3) e^{(n)} / \left[\kappa(n) - \kappa(n-1)\right] \quad (1)$$

where n is the number of multi-component spectrum splitting and κ the wavenumber. In case of non-equilibrium turbulence issued from the non-linear interaction between the coherent structures and the random turbulence, that displays the slope and shape modification of the energy spectrum,

$$E\left(\kappa(n)\right) = \left(\gamma_\kappa \alpha_n\right)^{-(2/5).(p)} \left[1 - \kappa(n-1)/\kappa(n)\right] (-p) e^{(n)} / \left[\kappa(n) - \kappa(n-1)\right] \quad (2)$$

where $-p \neq -5/3$.

Whenever only one organised mode arises, $n = 1$ and k is the wavenumber. By means of the experimental study of Braza et al. [3], it has been found that the velocity scale $k^{0.5}$ (k is the turbulence kinetic energy) is reduced by a factor of 4.5 in respect of the non-equilibrium regions. This corresponds to a reduction of the length scale by 0.22 in the non-equilibrium regions, comparing with the equilibrium turbulence length scale $l_{RANS} = k^{3/2}/\epsilon$. According to the relation $\nu_t = C_\mu k^{0.5} l$, the equivalent eddy-diffusion coefficient C_μ takes the value of 0.02.

This fact has been also shown by means of the DRSM modeling, (Bouhadji et al. [2]) where the eddy-diffusion C_μ coefficient was derived by the Launder, Reece, Rodi second-order closure, [9], involving Shima's damping function at the vicinity of the wall, [10]. The test-case of a NACA0012 airfoil at 20° and at Reynolds number 10^5 has been considered (Berton et al. [1]). The turbulence anisotropy tensor has been evaluated in the unsteady boundary layer and in the detached region by means of the DNS study of IMFT (Hoarau et al. [8]). Figure 2 shows that the diagonal term of the turbulent stress anisotropy, $b_{12} = -uv/k$ is not constant and much lower than in equilibrium boundary layers, ($b_{12} \approx 0.30$ and practically constant). Furthermore, the second-order moment closure provides the variations of an equivalent eddy-diffusion coefficient, (table 2.) that indicates a slight dispersion in the variation of the C_μ whose values are of an order of magnitude of 0.02, whereas the equilibrium turbulence value is 0.09.

X/C	Y/C	C_μ
0.3610^{-1}	0.3210^{-1}	0.0158
0.45	0.5710^{-1}	0.01859
0.9064	0.1510^{-1}	0.01938
1.41	-0.678	0.0178
1.23	0.11	0.0172
0.73	0.19	0.024

Table 1. evaluation of an equivalent C_μ coefficient by means of the DRSM (LRR); NACA0012 wing, $\alpha = 20°$, $Re = 10^5$

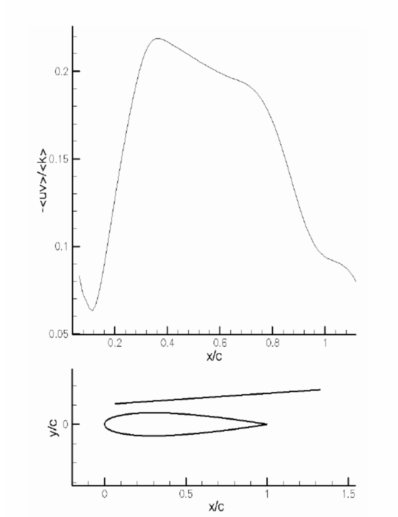

Figure 2. mean velocity profile in the recirculation region, Berton et al. [1]

2.1. OES approach

The above considerations have been done in the context of a suitable turbulence spectrum splitting to predict turbulent flows with coherent structures, in presence of solid walls. According to the Organised Eddy Simulation approach (Dervieux et al. [4]), the physical domain is decomposed on two parts: the coherent part to be resolved, and the random part to be modelled by advanced statistical turbulence modelling, efficient in high-Re unsteady wall flows (figure 3).

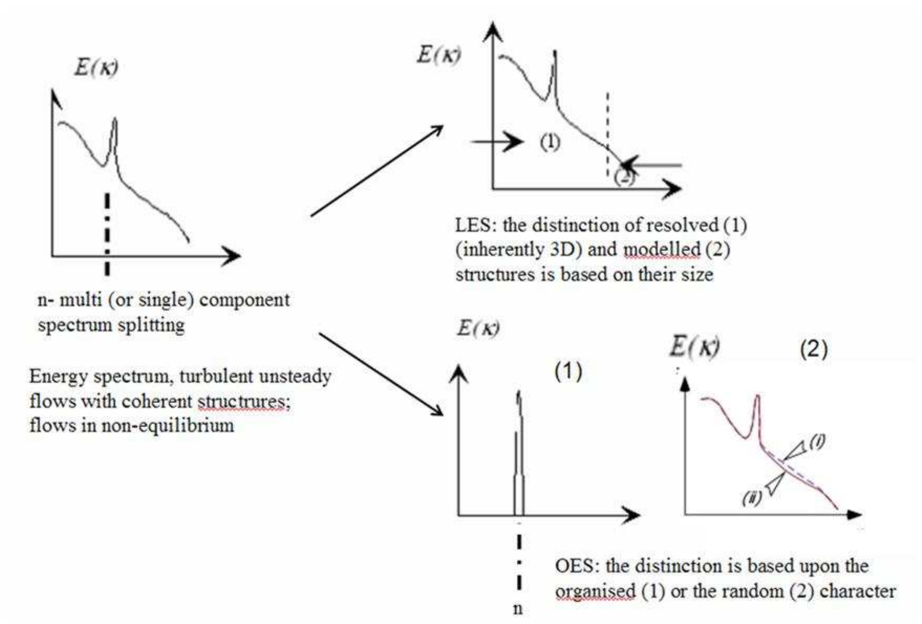

Figure 3. schematic representation of the energy spectrum in the URANS/OES approach

2.2. DES approach

In the Detached Eddy Simulation approach, the turbulence length scale in the energy transport equation is chosen as the minimum between a RANS and a LES length scale. Around the obstacle, the RANS scale is choosen as a result of this assumption, where the LES scale is applied in the detached regions:

$$l_{DES} = min\,(l_{RANS}, C_{DES} \times \Delta) \tag{3}$$

where C_{DES} is the DES constant calibrated by means of homogeneous, isotropic turbulence spectrum, and Δ is the largest dimension of the elementary control volume cell, $\Delta = max\,(\Delta_x, \Delta_y, \Delta_z)$. As an example, for the one-equation Spalart-Allmaras model ([11]),

$$l_{DES} = min\,(d_\omega, C_{DES} \times \Delta) \tag{4}$$

where d_ω is the distance from the wall. The modification of the length scale has a consequence the augmentation of the dissipation term in the eddy-viscosity transport equation:

$$D^\nu = \left(C_{\omega 1} f\omega - \frac{C_{b1}}{\kappa^2} f_{t2}\right)\left(\frac{\tilde{v}}{l_{DES}}\right)^2 \tag{5}$$

In the $k-\omega$ model,

$$l_{DES} = min\left(k^{1/2}/\beta\omega, C_{DES} \times \Delta\right) \tag{6}$$

As a consequence, the dissipation term in the kinetic energy transport equation increases:

$$D^k = \frac{\rho k^{3/2}}{l_{DES}} \tag{7}$$

In the case of coherent structures formation in the vicinity of the wall, and in respect of the previous paragraph discussion, the region around the obstacle is drastically submitted to non-equilibrium turbulence effects, that yield modification of the URANS length scale. This needs a further reduction of the turbulence kinetic energy as discussed above, that is reached by using the l_{OES} length scale,

$$l_{OES} = \frac{k^{1/2}}{C_\mu \omega} \tag{8}$$

with the reduced C_μ value.

In the present paper, the flow around a NACA0021 airfoil at 60° is studied by means of the DES-Spalart-Allmaras (DES-SPA), Spalart and Allmaras [11], the DES-$k-\omega$ and the DES/OES-$k-\omega$.

3. Flow around NACA0021

NACA0021 airfoil at angle of attack 60° is studied at the Reynolds number based on the chord length $Re = \frac{U_\infty C}{\nu} = 2.7 \times 10^5$, Swalwell et al. [12]. The NSMB code (Navier-Stokes Multi-Block) has been employed. The advective terms have been discretised by the Roe sheme and the diffusion terms by central differences. A fourth-order Range-Kutta scheme has been employed for the time derivatives.Two grids are used: 8 blocks, $148 \times 104 \times 35$ (538.720) nodes for the 1 chord spanwise length case, and 64 blocks, $148 \times 104 \times 135$ (2.077.920) nodes for the 4C case, figure 4. Dimensionless time step is about 2.4 10-3.

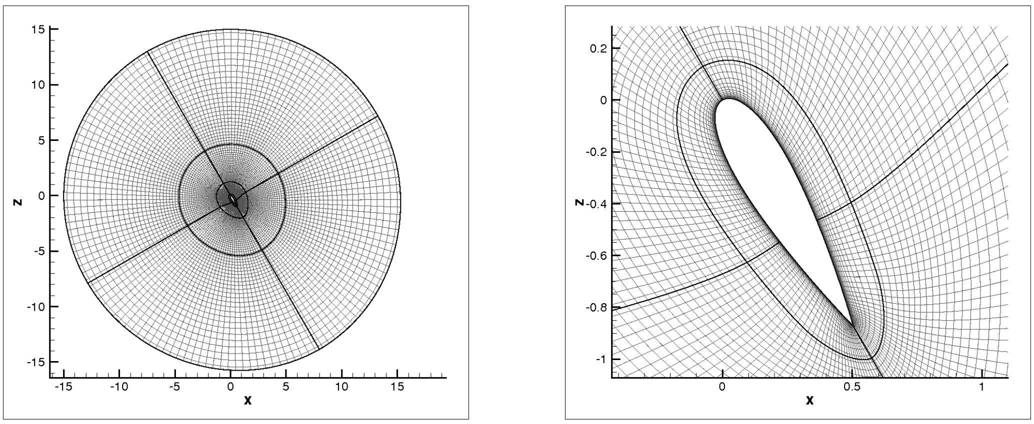

Figure 4. computational grid

Table 2 shows the mean global parameters in comparison with experimental results. The DES/OES modelling approach provide a good comparison. The dimensionless frequency (Strouhal number) is of order of 0.186 (0.2 in the experiment). A good comparison is also shown in figure 5 representing the time- and span-averaged wall pressure coefficient.

NACA0021	DES- SPA	DES-$k-\omega$	DES/OES -$k-\omega$	Exp
C_D	1.851	1.796	1.682	1.547
C_L	1.106	1.093	1.002	0.931

Table 2. global parameters in comparison with experimental data

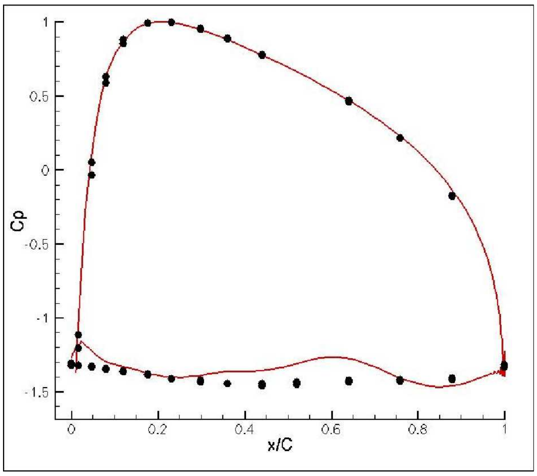

Figure 5. time- and span- averaged C_p, DES- $k-\omega$ model, comparison with experimental data

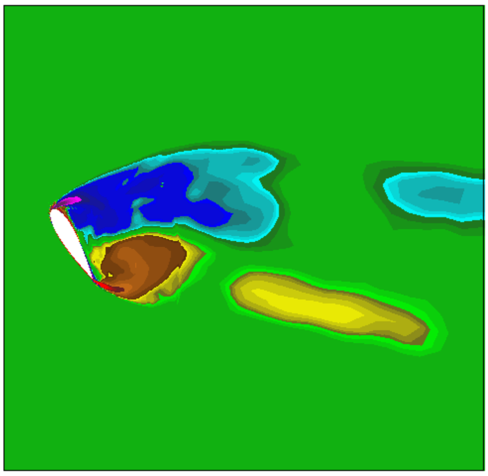

Figure 6. DES- $k-\omega$ model, iso-vorticity contours of time- and span- averaged field over one period

Figures 7 and 8 show instantaneous flow fields for the DES-SPL and DES/OES- $k-\omega$ respectively. The phase angle fields, figure 9 show the alternating Von-Kármán vortex shedding, as well as the smaller scale vortex motion within a period of the main vortex shedding. Figure 11 shows the time ans span- averaged field by the DES- $k-\omega$ model; In addition to the two main lobes, smaller scale structures are shown at the leading and trailing edges.

4. Conclusion

This paper presents a numerical simulation of strongly detached 3D flow around a NACA0021 airfoil at high angle of attack. The performances of suitable DES

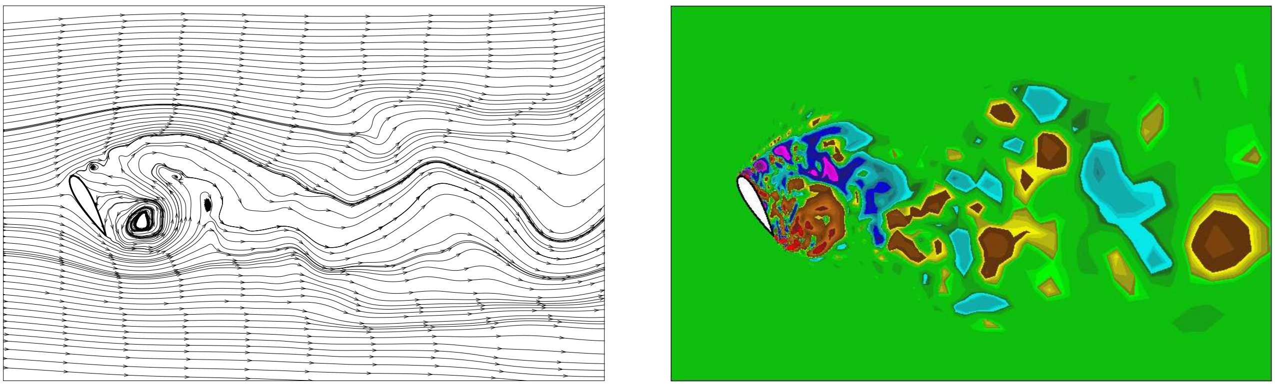

Figure 7. streamlines and iso-vorticity contours, median plane, DES-SPL model

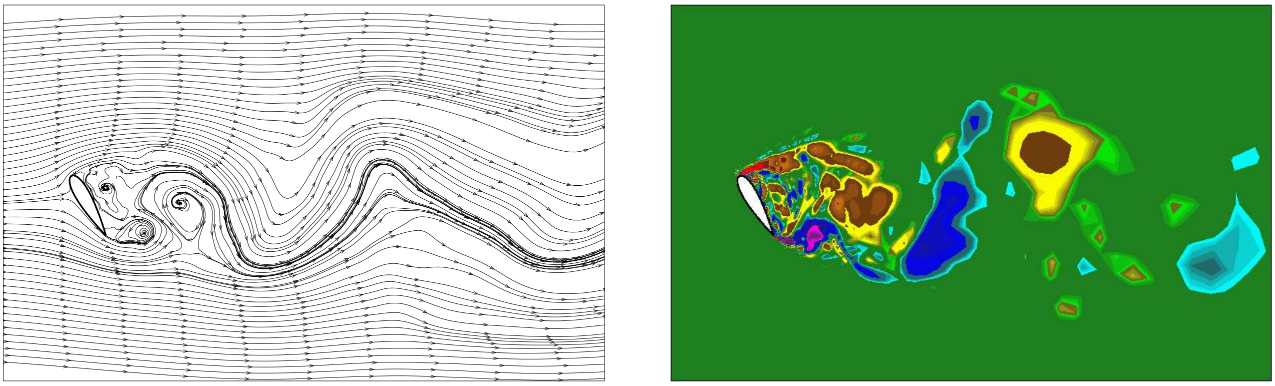

Figure 8. streamlines and iso-vorticity contours, median plane, DES/OES-$k-\omega$ model

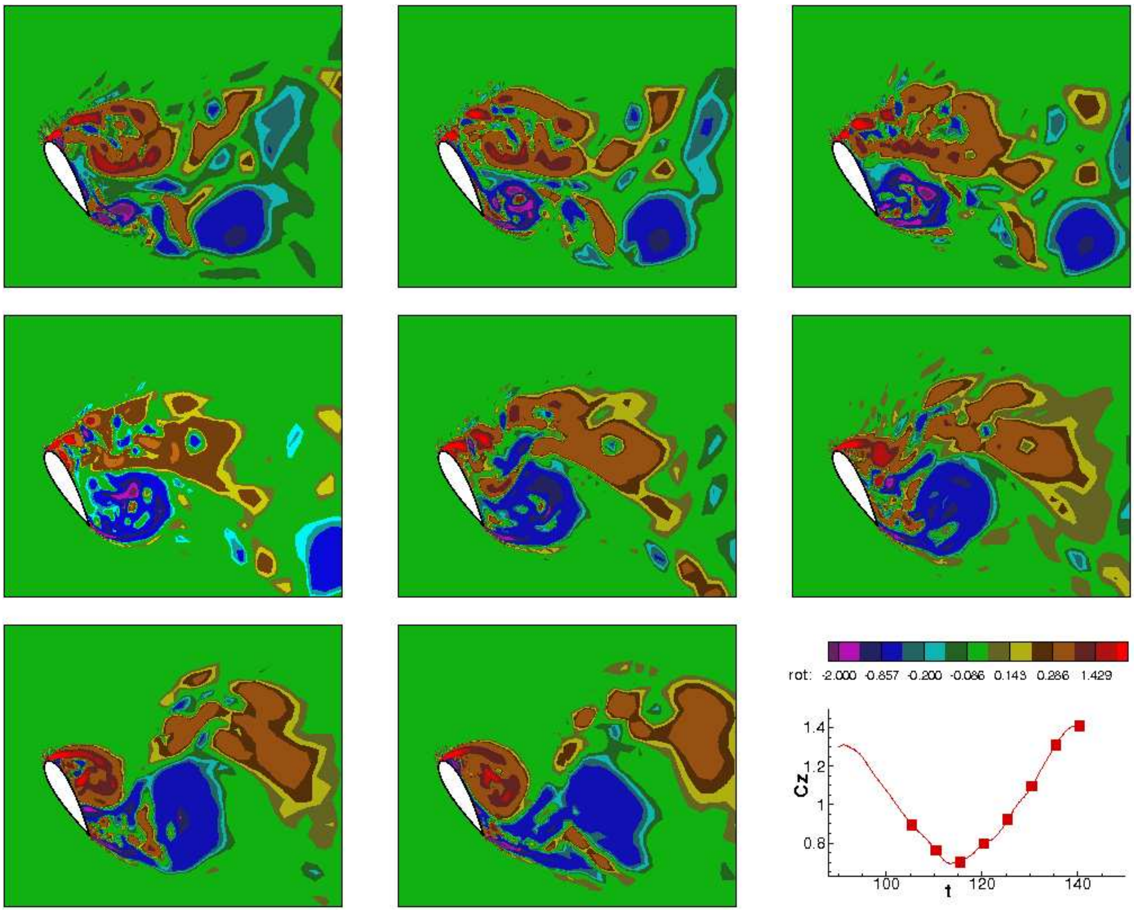

Figure 9. DES- $k-\omega$ model, time evolution of the flow over a period of the main vortex shedding

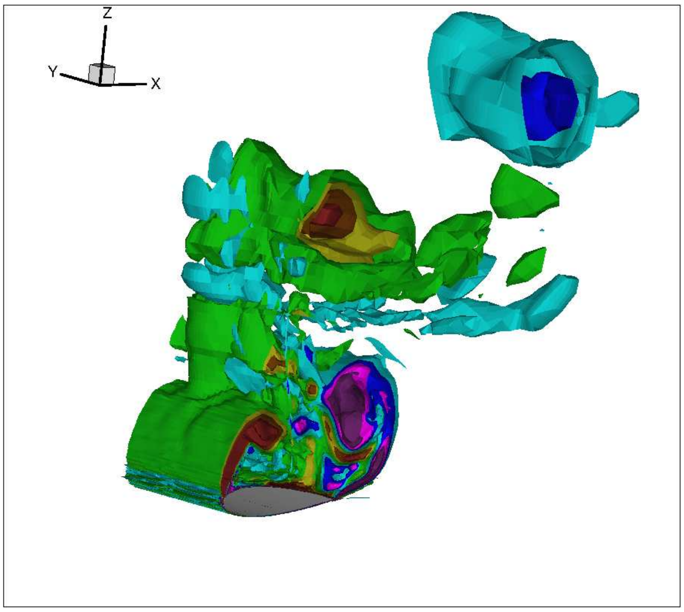

Figure 10. DES- $k - \omega$ model, 3D iso-vorticity surfaces, 1C spanwise length case

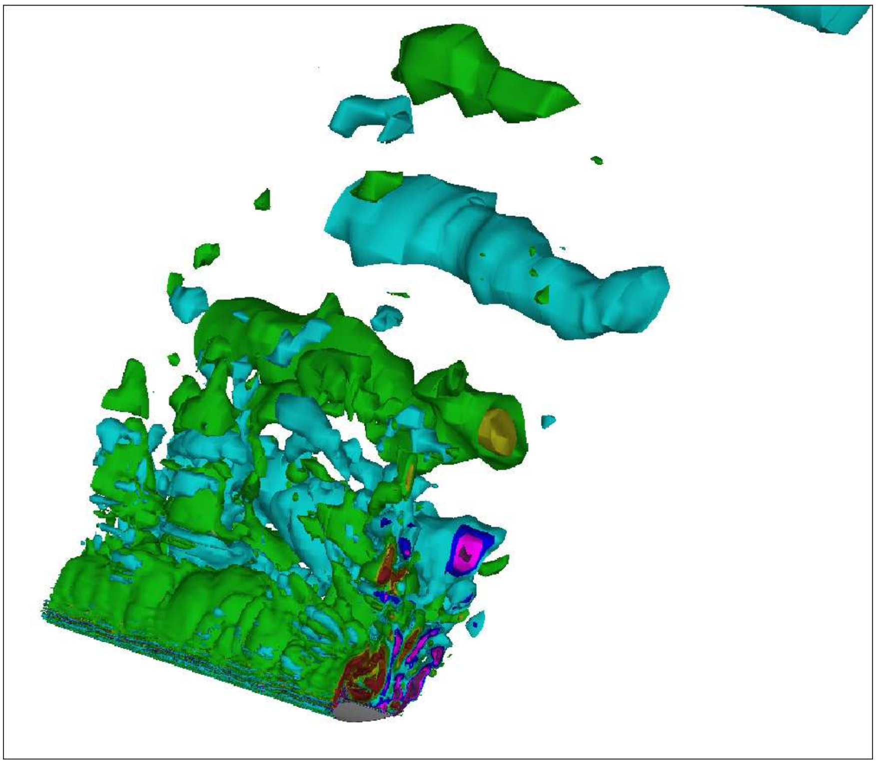

Figure 11. DES/OES- $k - \omega$ model, 3D iso-vorticity surfaces, 3C spanwise length case

approaches are shown for the prediction of the global and local parameters. It has been shown that the OES approach is appropriate for the prediction of this kind of flows. In our current developments the OES approach is extended in a tensorial basis for the eddy viscosity, reinforcing the prediction of normal stress anisotropy near the wall.

Acknowledgements

This work has been carried out in the research group EMT2 (Ecoulements Monophasiques, Transitionnels et Turbulents) of the Institut de Mécanique des Fluides de Toulouse. Part of this work is carried out on the basis of CPU allocations of the national computer centres of France CINES, CALMIP and IDRIS. This study is part of the European program DESIDER, N AST3-CT-2003-502842, coordinated by EADS.

References

[1] E. Berton, C. Allain, D. Favier, and C. Maresca. Experimental methods for subsonic flow measurements. *Notes on Num. Fluid Mech. and Multidisciplinary Design*, 81:251–260, 2002. dedicated volume in "Progress in Computational Flow-Structure Interaction".

[2] A. Bouhadji, S. Bourdet, M. Braza, Y. Hoarau, P. Rodes, and G.Tzabiras. Turbulence modelling of unsteady flows with a pronounced periodic character. *Notes on Num. Fluid Mech. and Multidisciplinary Design*, 81:87–96, 2002. dedicated volume in "Progress in Computational Flow-Structure Interaction".

[3] M. Braza, R. Perrin, and Y. Hoarau. Turbulence properties in the cylinder wake at high reynolds number. *J. Fluids Struct.*, 22:757–771, 2006.

[4] A. Dervieux, M. Braza, and J.P. Dussauge. Computation and comparison of efficient turbulence models for aeronautics-european research project ETMA. Notes on Num. Fluid Mech., Vol65, Ed. Vieweg, 1998.

[5] H. Djeridi, M. Braza, R. Perrin, G. Harran, E. Cid, and S. Cazin. Near-wake turbulence properties around a circular cylinder at high reynolds number. *J. Flow Turbulence and Combustion*, 71:19–34, 2003.

[6] J.O. Hinze. *Turbulence.* Mc Graw-Hill, second edition, New-York,USA, 1975.

[7] Y. Hoarau and M. Braza. Note on the organised eddy simulation equilibrium and non-equilibrium turbulence regions. 2002.

[8] Y. Hoarau, D. Faghani, M. Braza, R. Perrin, D. Anne-Archard, and D. Ruiz. Direct numerical simulation of the three-dimensional transition to turbulence in the incompressible flow around a wing. *J. Flow Turbulence and Combustion*, 71:119–132, 2003.

[9] B. E. Launder, G. J. Reece, and W. Rodi. Progress in the development of a reynolds stress turbulence closure. *J. Fluid Mech.*, 68:537–566, 1975.

[10] N. Shima. A reynolds-stress model for near-wall and low-reynolds number regions. *J. Fluids Eng.*, 110:38–44, 1988.

[11] P.R. Spalart and S.R. Allmaras. A one-equation turbulence models for aerodynamic flows. *AIAA paper*, (92-0439), 1992. 30^{th} Aerospace Sciences Meeting - Reno, Nevada.

[12] K. Swalwell, J. Sheridan, and W. Melbourne. Frequency analysis of surface pressures on an airfoil after stall. *AIAA Applied Aerodynamics Conference*, 2003.